

Published in final edited form as:

J Biol Chem. 2005 April 8; 280(14): 13624–13630.

CALMODULIN IS REQUIRED FOR VASOPRESSIN-STIMULATED INCREASE IN CYCLIC AMP PRODUCTION IN INNER MEDULLARY COLLECTING DUCT

Jason D Hoffert, Chung-Lin Chou, Robert A Fenton, and Mark A Knepper

From the Laboratory of Kidney and Electrolyte Metabolism, NHLBI, National Institutes of Health, Bethesda, MD 20892

Abstract

Calmodulin plays a critical role in regulation of renal collecting duct water permeability by vasopressin. However, specific targets for calmodulin action have not been thoroughly addressed. In the present study, we investigated whether Ca^{+2} /calmodulin regulates adenylyl cyclase activity in the renal inner medullary collecting duct. Rat inner medullary collecting duct suspensions were incubated in the presence or absence of 0.1 nM vasopressin and the calmodulin inhibitors, monodansylcadaverine, W-7, and trifluoperazine followed by measurement of cAMP. Vasopressin-stimulated cAMP elevation was significantly attenuated in the presence of calmodulin inhibitors. Analysis of transglutaminase 2 knockout mice confirmed that these compounds were not acting through inhibition of transglutaminase 2 activity. Calmodulin inhibitors also blocked both cholera toxin- and forskolin-stimulated cAMP accumulation. In isolated perfused tubules, W-7 reversibly blocked vasopressin-stimulated urea permeability, a process that requires a rise in intracellular cAMP, but does not appear to involve protein trafficking to the apical plasma membrane. These results suggest that calmodulin is required for vasopressin-stimulated adenylyl cyclase activity in intact inner medullary collecting duct. RT-PCR, immunoblotting, and immunohistochemistry revealed the presence of the calmodulin-sensitive adenylyl cyclase type 3 in rat collecting duct, an isoform previously not known to be expressed in collecting duct. Long-term treatment of Brattleboro rats with a vasopressin analog markedly decreased adenylyl cyclase type 3 protein abundance, providing an explanation for long-term downregulation of vasopressin response in collecting duct. These studies demonstrate the importance of calmodulin in the regulation of collecting duct adenylyl cyclase activity and transport function.

The collecting duct portion of the mammalian renal tubule regulates water and solute transport via the action of the antidiuretic hormone arginine vasopressin (AVP). AVP is released from the posterior pituitary in response to elevated plasma osmolality and binds to V2 receptors on the basolateral surface of the collecting duct epithelium, triggering a G-protein-linked signaling cascade which leads to elevation of cyclic AMP (cAMP) and water channel aquaporin-2 (AQP2) vesicle insertion into the apical plasma membrane (1). Recently we demonstrated that calmodulin (CaM), a ubiquitous Ca^{+2} -binding protein, is required for AQP2 vesicle trafficking in response to vasopressin stimulation (2). Preincubation of isolated perfused rat inner

Address correspondence to: Mark A. Knepper, M.D. Ph.D., National Institutes of Health Bldg. 10, Room 6N260, 10 CENTER DR MSC 1603, BETHESDA, MD 20892-1603, Phone: (301)496-3064, FAX (301)402-1443, e-mail: knep@helix.nih.gov.

This study was funded by the Intramural Budget of the National Heart, Lung, and Blood Institute (National Institutes of Health, project no. Z01-HL-01282-KE to M. A. Knepper).

Abbreviations: IMCD, inner medullary collecting duct; CaM, calmodulin; AC, adenylyl cyclase; AVP, [Arg8]vasopressin; dDAVP, [deamino-Cys1,D-Arg8]vasopressin; AQP, aquaporin; cAMP, cyclic adenosine monophosphate; CTX, cholera toxin; MDC, monodansylcadaverine; TFP, trifluoperazine; DTT, dithiothreitol; PBS, phosphate-buffered saline; BCA, bicinchoninic acid; IBMX, isobutyl methylxanthine; RT-PCR, reverse transcription-polymerase chain reaction; DMSO, dimethyl sulfoxide..

medullary collecting duct (IMCD) with the CaM inhibitors W-7 and trifluoperazine (TFP) blocked AVP-stimulated water permeability. Further investigation revealed that CaM activates myosin light chain kinase (MLCK) and subsequent non-muscle myosin II-dependent vesicle trafficking of AQP2 (3).

In this paper, we sought to identify a role for CaM in regulating more proximal events in the collecting duct response to vasopressin, which could have an effect on other collecting duct functions including urea and Na⁺ transport. Given the fact that CaM is known to regulate a wide range of cellular processes, it is reasonable to assume that this protein could act at multiple levels in the vasopressin signaling pathway. One of the major secondary messengers that is increased in response to AVP is cAMP. Elevation of cAMP is required for AQP2 vesicle exocytosis (4) as well as the corresponding increase in collecting duct water permeability (5). Other collecting duct proteins regulated by cAMP include urea transporter UT-A1 (6) and the epithelial sodium channel (ENaC) (7).

Measuring cAMP in enriched IMCD fractions, we found that elevation of cAMP in response to AVP requires CaM. Further analysis suggested that CaM is acting at the level of adenylyl cyclase. This is the first demonstration of CaM-dependent cAMP accumulation in response to AVP in intact IMCD tubules, which supports prior conclusions from studies in cultured LLC-PK₁ cells (8) and mouse outer medulla (9). In addition, we present evidence showing that CaM is required for AVP-mediated urea permeability in isolated perfused IMCD, another process that is cAMP-dependent (10), suggesting that CaM may play a broader regulatory role in the collecting duct than initially thought.

We utilized RT-PCR, immunoblotting, and immunohistochemistry to look for the presence of a CaM-sensitive adenylyl cyclase (AC) isoform in IMCD cells. Of the 9 mammalian AC isoforms identified, three have been shown to be calmodulin sensitive: AC1, AC3, and AC8 (11). AC1 and 8 are expressed mainly in tissues of the central nervous system, whereas AC3 has a broader profile, having been found in olfactory neuroepithelium (12), testes (13), brown adipose tissue (14), and uterus (15). Our studies demonstrated the presence of a single CaM-sensitive adenylyl cyclase isoform in IMCD, namely AC3. In collecting duct, AC3 may act as the target cyclase for Ca⁺²/CaM-dependent cAMP accumulation in response to vasopressin.

MATERIALS AND METHODS

Animals.

Pathogen-free male Sprague-Dawley rats (Taconic Farm Inc. Germantown, NY) were maintained on an autoclaved pelleted rodent chow (413110-75-56, Zeigler Bros., Gardners, PA) and *ad libitum* drinking water. All experiments were conducted in accord with an animal protocol approved by the Animal Care and Use Committee of the National Heart, Lung, and Blood Institute (ACUC protocol number 2-KE-3). Transglutaminase 2 (TG2) knockout mice and wildtype mixed background mice, a kind gift of Dr. Gerry Melino (University of Roma, Italy) (16), were maintained on the same autoclaved pelleted rodent chow and *ad libitum* drinking water. Immunoblotting as well as PCR amplification of tail genomic DNA were used to distinguish knockout from wildtype mice. All mouse experiments were conducted in accord with animal protocol H-0047 approved by the Animal Care and Use Committee of the National Heart, Lung, and Blood Institute.

Materials.

Monodansylcadaverine (MDC), trifluoperazine (TFP), forskolin, and cholera toxin (CTX) were from Sigma. W-7 was from Calbiochem. Cyclic AMP enzyme immunoassay kit was from Cayman Chemical. Adenylyl cyclase antibodies, ACIII (C-20; sc-588) and ACV/VI (C-17;

sc-590), were from Santa Cruz Biotech and used at the manufacturer's recommended dilutions. Both affinity-purified aquaporin-1 (L266) (17) and aquaporin-2 (L127) (18) antibodies have been described.

IMCD suspensions.

IMCD suspensions were prepared from inner medulla of rat kidney using the method of Stokes et al. (19) with some modifications (20). Briefly, rats were killed by decapitation and whole inner medullas were removed and finely minced with a razor blade. Minced tissue was incubated for 90 min at 37°C with gentle agitation in a collagenase/hyaluronidase solution to dissociate individual tubule segments. After incubation, the sample was centrifuged at 80 g for 30 sec to enrich for heavier IMCD structures, followed by centrifugation of the supernatant at 1,500 g for 5 min to pellet the lighter non-IMCD fragments. Pellets were resuspended in either bicarbonate buffer (NaCl 118 mM, NaHCO₃ 25 mM, KCl 5 mM, Na₂HPO₄ 4 mM, MgSO₄ 1.2 mM, CaCl₂ 2 mM, glucose 5.5 mM) for measurement of cAMP or in Laemmli buffer for immunoblotting.

Measurement of cAMP.

Fifty microliter aliquots of IMCD suspensions were preincubated at 37°C for 10 min with 0.5 mM IBMX in the presence or absence of various CaM inhibitors, followed by incubation with 0.1 nM AVP for 5 min. Samples were pelleted at 1000 g for 1 min and the supernatant discarded. Tissue pellets were lysed by adding 0.2 N HCl and incubating for 20 min at RT, followed by centrifugation at > 10,000 g for 10 min. Supernatants were saved for measurement of cAMP and pellets were used to measure protein content (BCA assay, Pierce). cAMP content was measured using a non-radioactive enzyme immunoassay kit (Cayman Chemical, Ann Arbor, MI) based on competitive binding between endogenous cAMP and an exogenous cAMP-tagged acetylcholinesterase tracer. Samples were run in 96-well microtiter plate format and measured at $\lambda = 414$ nm on a plate reader (Labsystems Multiskan MCC/340). Absorbance data was analyzed using a spreadsheet program provided by Cayman Chemical which calculated cAMP content in pmol/ml. This value was then normalized to total protein which had been previously measured using the BCA assay. The final value was expressed as fmol cAMP/ μ g protein.

Isolated perfused IMCD tubules.

IMCD segments were microdissected from the midregion of the inner medulla (40–70% of the distance from the inner-outer medullary junction to the papillary tip of the rat kidney). The tubules were transferred to a perfusion chamber, mounted on an inverted microscope, cannulated by concentric pipettes, and perfused *in vitro*. The perfusate and the peritubular bath solutions were identical to the dissection solution except that in the bath solution 5 mM creatinine was replaced by 5 mM urea. The urea permeability was determined by measuring the urea flux resulting from the transepithelial urea gradient. The urea concentrations in the perfusate, bath, and collected fluid were measured fluorometrically using a continuous-flow ultramicrofluorometer and an enzymatic assay (Infinity Urea Nitrogen reagent, Cat no. TR12321, ThermoTrace).

RT-PCR.

Total RNA was isolated from rat IMCD and brain using the guanidinium thiocyanate/cesium-TFA method. Potential contaminating genomic DNA was removed from the RNA preparations by a 30-min incubation with DNase I (DNA-free, Ambion). Total RNA (1 μ g) was reverse transcribed using oligo(dT) and Superscript II RT (Invitrogen) following the manufacturer's recommended protocol. RT-negative controls were performed to assess the presence of possible genomic DNA contamination of RNA samples. PCR primers were designed against

the corresponding cDNAs of rat adenylyl cyclases 1–9 in order to generate products of approximately 200–500 bp in size. All primers were designed to span at least one intronic region in order to distinguish possible amplification of genomic DNA. All amplified products were confirmed by sequencing.

dDAVP infusion.

Under methoxyflurane anesthesia (Metofane; Pitman-Moore, Mundelein, IL), osmotic minipumps (model 2002; Alzet, Palo Alto, CA) were implanted subcutaneously in Brattleboro rats to deliver 20 ng/h of dDAVP (Rhone-Poulenc Rorer, Collegeville, PA), a V_2 vasopressin receptor-selective agonist. Brattleboro rats used as controls were implanted with minipumps containing vehicle (saline) alone. After 7 days of dDAVP or vehicle infusion, during which time rats received water and pelleted chow ad libitum, all rats were killed by decapitation.

Immunoblotting.

Tissue samples were homogenized in isolation solution (10 mM Triethanolamine, 250 mM sucrose, pH adjusted to 7.6, Roche protease inhibitor tablet) using a mechanical tissue grinder (OMNI International) and total protein concentration was determined by the BCA assay (Pierce) using BSA as the standard. Samples were then solubilized in Laemmli buffer (10 mM Tris pH 6.8, 1.5% SDS, 6% glycerol, 0.05% bromophenol blue, and 40 mM DTT). 15–50 μ g of protein was subjected to SDS-PAGE (21) and immunoblotting as described (22).

Immunohistochemistry.

Rat kidneys were perfusion fixed, paraffin embedded, and processed for immunostaining via horseradish peroxidase as described (23).

Statistics.

Quantitation of changes in cAMP as well as densitometric analysis of protein immunoblots are expressed as the mean \pm SE ($n \geq 3$) for each group. Unpaired t-tests and ANOVA were performed as appropriate for the given data set.

RESULTS

Effect of calmodulin (CaM) inhibition on AVP-stimulated cAMP accumulation in rat IMCD.

In order to address the role of CaM in regulating cAMP production in response to vasopressin, we incubated rat IMCD cell suspensions with three different CaM inhibitors: monodansylcadaverine (MDC) (24), W-7 (25), and trifluoperazine (TFP) (26). Following a 10 min preincubation period with these compounds in the presence of the phosphodiesterase inhibitor IBMX (0.5 mM), 0.1 nM AVP or vehicle (bicarbonate buffer) was added to the tubules for 5 min. cAMP content was subsequently measured by a non-radioactive enzyme immunoassay as described in *Methods*. cAMP levels were significantly increased 4–5 fold in IMCD suspensions incubated with AVP alone (Fig. 1A,B). Preincubation of tubules with MDC (200 μ M) completely abolished AVP-stimulated cAMP accumulation in IMCD cells [61.2 ± 17.5 vs. 529.3 ± 52.7 (AVP alone) fmol cAMP/ μ g of protein] (Fig. 1A). Preincubation of tubules with two other CaM inhibitors, W-7 (25 μ M) [165.4 ± 33.1 vs. 378.5 ± 19.2 (AVP alone) fmol/ μ g] and TFP (30 μ M) [174.5 ± 37.4 vs. 378.5 ± 19.2 (AVP alone) fmol/ μ g], also significantly reduced the increase in cAMP due to AVP treatment. Increasing the concentration of these drugs to 100 μ M gave an even greater inhibition (Fig. 1B), demonstrating the dose-dependence of this phenomenon.

CaM inhibitors act at the level of adenylyl cyclase.

Although our results indicated that CaM was required for elevation of cAMP by vasopressin, it was unclear at what level CaM was affecting the signaling pathway (e.g. V2 receptor, G_s , or adenylyl cyclase). Incubation of IMCD suspensions with cholera toxin (CTX) at 1 $\mu\text{g/ml}$, a potent ADP-ribosyltransferase which causes persistent activation of G_{sa} , produced a 4.6-fold increase in cAMP that was blocked by either W-7 (25 μM) or TFP (30 μM) (Fig. 2A). The fact that CaM inhibitors block CTX-mediated cAMP elevation rules out the V2 receptor as the site of action of Ca^{+2} /CaM, and suggests that CaM is probably acting either at the level of G_{sa} or of the adenylyl cyclase responsible for cAMP production in the IMCD.

Forskolin is a direct activator of nearly all known adenylyl cyclase isoforms (11). Treatment of IMCD cells with forskolin (1 μM) resulted in a nearly 10-fold increase in cAMP, which was significantly decreased by preincubation with MDC [638.3 ± 45.3 vs. 2076 ± 390.4 (forskolin alone) fmol/ μg (Fig. 2). Similar results were obtained when tubules were preincubated with W-7 or TFP prior to stimulation with forskolin (data not shown). These results indicate that CaM is acting beyond the level of G_{sa} , viz. on the adenylyl cyclase responsible for most cellular cAMP production itself.

Effect of MDC on cAMP accumulation in wildtype and transglutaminase 2 (TG2) knockout mice.

Previous studies have shown that both MDC and W-7 can inhibit transglutaminase in addition to calmodulin (24;27). Both MDC and W-7 possess a high degree of structural similarity (Fig. 3) and can act as primary amine substrates for crosslinking by transglutaminase. To determine whether these inhibitors are acting through transglutaminase, we obtained transglutaminase 2 (TG2) knockout mice (Dr. Gerry Melino, University of Roma (16)), which lack both transcript and protein for the major isoform expressed in IMCD (unpublished observations). IMCD from wildtype mixed background and TG2 ($-/-$) mice produced similarly elevated levels of cAMP in response to AVP (Fig. 4). Preincubation with MDC blocked AVP-induced cAMP responses in both wildtype and TG2 ($-/-$) mice to a similar extent, suggesting that these inhibitors are not acting through promiscuous inhibition of transglutaminase and that transglutaminase activity is not required for elevation of cAMP by vasopressin.

Effect of CaM inhibition on AVP-stimulated urea permeability in isolated perfused rat IMCD.

Both vasopressin-stimulated water and urea permeability in IMCD require elevation of intracellular cAMP. Our previous studies have demonstrated a clear role of calmodulin in regulation of water permeability at the level of aquaporin trafficking (2;3); however, no clear role for calmodulin had been identified for AVP-stimulated urea permeability. To address this, we isolated rat IMCD segments by microdissection and utilized the perfused tubule method described in *Methods* to measure changes in collecting duct urea permeability in response to AVP. The urea permeability of isolated tubules was increased following addition of 0.1 nM AVP to the bath solution [45.7 ± 0.9 (basal) vs. 116.7 ± 19.2 (AVP) $\times 10^{-5}$ cm/s] (Fig. 5). Subsequent addition of W-7 (25 μM) dramatically reduced urea permeability to basal levels [AVP + W-7 = $26.3 \pm 11.3 \times 10^{-5}$ cm/s]. Addition of W-7 prior to stimulation with AVP also reduced urea permeability [14.7 ± 3.8 (W-7) vs. 21.7 ± 5.8 (W-7 + AVP) $\times 10^{-5}$ cm/s]. More importantly, urea permeability increased upon washout of W-7 with fresh AVP solution [AVP washout = 92.0 ± 7.8], demonstrating the reversibility of this process.

Identification of adenylyl cyclase isoforms in rat IMCD by RT-PCR.

To determine which isoforms of adenylyl cyclase are present in rat IMCD, specific primer sets were generated for each AC isoform (1–9) using sequences obtained from the full length cDNA of the corresponding gene. Total RNA was extracted from tissue and used for reverse

transcription reactions in the presence or absence of reverse transcriptase (RT +, RT – respectively; Fig. 6), followed by amplification by PCR. Rat brain was utilized as a positive control for all primer sets, and bands of the appropriate size were present for each AC isoform (*top panel*, Fig. 6). In all reactions without RT, the band is absent. This eliminates the possibility that bands in RT + reactions represent amplified contaminating genomic DNA. Analysis of rat IMCD revealed the presence of the majority of AC isoforms except AC1 and 8 (*bottom panel*, Fig. 6). Most importantly, the only CaM-stimulated isoform of adenylyl cyclase detectable by RT-PCR was AC3. *Adenylyl cyclase 3 (AC3) is enriched in IMCD cells*. Rat inner medullas were processed according to *Methods* to generate two fractions: IMCD cells and non-IMCD cells. The former is enriched in collecting duct fragments, the latter possesses mainly thin limb segments and *vasa recta*. To assess the level of enrichment, protein lysates from each fraction were analyzed by immunoblotting for aquaporin-1 (AQP1), a water channel present in thin descending limbs and vasculature but absent from IMCD. As expected, AQP1 was much more abundant in the non-IMCD fraction. The immunoblot band densities for AQP1 were increased 5.4-fold in non-IMCD fractions compared to IMCD fractions ($P < 0.001$; $n = 3$) (Fig. 7A), suggesting that the IMCD pellet is devoid of a large amount of contaminating non-IMCD material. An affinity-purified rabbit polyclonal AC3 antibody recognized two distinct bands between 160 and 250 kDa that were enriched 2.2-fold in IMCD fractions compared to non-IMCD ($P < 0.05$; $n=3$) (Fig. 7B). This antibody was raised against the highly divergent C-terminus of rat AC3 (PAAFPNGSSVTLPHQVVDNP; confirmed by mass spectrometry) and does not cross-react with ACs 1, 2, 4, 5, 6, and 9 (13). Both the number and size of bands is consistent with immunoblot results of AC3 expression in myenteric ganglia (28). In addition, these two bands, along with a smaller band under 160 kDa, were present in a sample of whole brain homogenate (Fig. 7B). All bands were absent with preadsorption of the AC3 blocking peptide (data not shown). The presence of AC3 protein on immunoblot supports the data generated by RT-PCR analysis and also demonstrates that this isoform is enriched in the collecting duct fraction of the inner medulla.

To further address the presence of AC3 in IMCD, we performed immunohistochemistry on rat inner medullary sections. AC3 was found in all IMCD cells, with a lower level of staining present in thin limb cells (Fig. 8A). This staining was largely ablated by preadsorption of the AC3 antibody with its corresponding blocking peptide (Fig. 8B). As expected AC6, the major isoform previously identified by RT-PCR in more proximal portions of the collecting duct (29) was also found in IMCD (Fig. 8C). We have previously demonstrated that AC6 protein is present in the IMCD by immunocytochemistry (30). Interestingly, both AC3 and AC6 appear to have similar distributions. Collecting duct staining was confirmed using an antibody to the collecting duct-specific marker protein aquaporin-2 (AQP2) (Fig. 8D). The presence of AC3 in IMCD directly demonstrates the presence of a Ca^{+2} /CaM-stimulated isoform in the IMCD and supports our conclusion that Ca^{+2} /CaM may act directly on adenylyl cyclase to enhance AVP-stimulated cAMP production.

Effect of long-term dDAVP administration on AC3 expression.

A prior study has shown that AC6 expression in collecting duct is reduced during long-term dDAVP treatment, thought to be the result of a conditioned “negative feedback” response (30). To address whether AC3 is similarly affected by dDAVP, Brattleboro rats were given dDAVP (20 ng/hr) or saline (control) via osmotic minipumps for 7 days, followed by isolation of inner medulla and immunoblotting. AQP2 was used as a positive control for the effect of dDAVP in collecting duct. AQP2 protein abundance was significantly increased 2.5 fold with dDAVP treatment (100 ± 2.7 control vs. 247.7 ± 8.6 dDAVP; $P < 1 \times 10^{-5}$) (Fig. 9, *bottom panel*). AC3 protein abundance decreased 2.9 fold (100 ± 12.3 control vs. 34.5 ± 8.6 dDAVP; $P < 0.01$) during long-term dDAVP treatment (Fig. 9, *top panel*). AC6 expression was reduced 5.0 fold (100 ± 11.7 control vs. 19.8 ± 2.9 dDAVP; $P < 0.0002$) (Fig. 9, *middle panel*). This

result suggests that AC3 and AC6 expression may be subject to similar long-term regulatory influences in IMCD cells.

DISCUSSION

Vasopressin acts via the V2 receptor (V2R) to increase water and urea permeability in the inner medullary collecting duct of the kidney. Water and urea are transported via different channels (31). Water transport occurs via AQP2 in the apical plasma membrane and aquaporins 3 and 4 in the basolateral plasma membrane (32). Regulation of water transport occurs via vasopressin-mediated AQP2 trafficking to the apical plasma membrane (33). Urea transport in the IMCD occurs via two urea channels, UT-A1 and UT-A3, present in the apical and basolateral plasma membrane respectively. The mechanism of urea transport regulation by vasopressin is not known, although it is believed that urea channels do not traffic to the apical plasma membrane together with AQP2 (34;35).

The regulation of both water and urea transport in the IMCD depends on activation of adenylyl cyclase activity via the heterotrimeric GTP-binding protein Gs (1). The molecular identity of the adenylyl cyclase responsible for vasopressin-mediated increases in cyclic AMP has not been previously addressed, although it has been widely assumed that type 6 adenylyl cyclase (AC6) is responsible for vasopressin-stimulated cAMP increases because it has been demonstrated to be relatively abundant in collecting duct principal cells (29;36). This isoform is inhibited by Ca^{+2} in the micromolar range (37) and is not calmodulin-sensitive (38). AC6 has been localized in the collecting duct by RT-PCR (29) and *in situ* hybridization (36). Furthermore, increasing intracellular calcium appears to inhibit AVP-stimulated cAMP in the outer medullary part of the collecting duct (29), supporting the conclusion that AC6 is responsible for vasopressin-dependent cAMP production by outer medullary collecting duct principal cells. However, earlier reports strongly suggest that vasopressin-sensitive renal epithelia possess CaM-sensitive AC activity. First, Ausiello *et al.* described CaM-stimulated adenylyl cyclase activity in a cell line sensitive to vasopressin (LLC-PK₁) (8). A subsequent study in microdissected outer medullary collecting ducts by Takaichi *et al.* (9) reported that AVP-sensitive cAMP production was CaM-dependent. Despite these findings, a candidate CaM-sensitive AC has not been found in the renal collecting duct.

In this study, we have identified a role for CaM in regulating the IMCD response to vasopressin at the level of adenylyl cyclase. Utilizing various CaM inhibitors, we were able to block AVP-dependent cAMP accumulation in both rat and mouse IMCD. Isolated perfused tubule experiments demonstrated that CaM is required for AVP-stimulated urea permeability in collecting duct, a process known to be cAMP-dependent. A recent paper demonstrated that CaM binds to the COOH-terminus of the V2R and mediates some of the actions of vasopressin (39). However, in the present study, CaM inhibitors also blocked the rise in cAMP in the presence of either cholera toxin or forskolin, providing strong evidence that CaM is acting directly on adenylyl cyclase to increase cAMP production.

What AC isoform could be responsible for CaM-dependent cAMP production in the IMCD? Three isoforms have been reported to be CaM-sensitive, namely AC1, AC3 and AC8 (11). Among these, we find evidence for the expression of only AC3 in the IMCD. Specifically, we have identified AC3 mRNA by RT-PCR in IMCD suspensions. Neither AC1 or AC8 transcripts were detectable in IMCD cells, even though these transcripts were readily detectable in brain with the same loading and amplification protocol. Furthermore, we find evidence for AC3 protein in IMCD through both immunoblotting and immunocytochemical studies. Ca^{+2} /CaM have been shown to stimulate AC3 activity in a number of systems including HEK-293 cell membranes (40) and bovine luteal cells (41). To our knowledge, this is the first demonstration of a CaM-stimulated isoform in collecting duct. Immunoblotting and immunohistochemistry

revealed that AC3 is enriched in IMCD cells compared with non-IMCD structures in the inner medulla, chiefly *vasa recta* and ascending and descending thin limbs of Henle. Long-term dDAVP administration in Brattleboro rats reduced expression of AC3 as well as AC6. A decrease in AC6 expression with dDAVP treatment has been reported previously (30). Reduced adenylyl cyclase expression may reflect a “negative feedback” mechanism that reduces cAMP after prolonged exposure to vasopressin. Taking into account this functional and expression data, we propose that AC3 is a target of CaM in IMCD cells and is, at least in part, responsible for the rise in cAMP in response to AVP.

Interestingly, our data indicate that both AC3 and the Ca^{+2} -inhibited isoform AC6 are expressed in the inner medullary collecting duct. Based on immunocytochemical labeling, it appears that both isoforms are expressed in the same cells. As yet it remains unclear what is the relative contribution of each isoform to the overall rise in cAMP during the stimulation of the collecting duct with AVP. The dramatic decrease in AVP-stimulated cAMP in the presence of the CaM inhibitors in our study suggests that the contribution of AC3 is quite significant under the conditions of the measurements. Previously, it was demonstrated that stimulation of inner medullary collecting ducts with AVP produces an increase in intracellular Ca^{+2} (10) via the V2 vasopressin receptor (42;43). The increase in intracellular Ca^{+2} is oscillatory in nature (44) and is dependent on Ca^{+2} release via ryanodine-sensitive stores (2). AC3 likely contributes to cAMP accumulation during periods of elevated intracellular Ca^{+2} when AC6, the Ca^{+2} -inhibited isoform, is probably in an inactive state. Conversely, AC6 may be the predominant producer of cyclic AMP when Ca^{+2} is low in the cell. Overall, the two isoforms in combination may provide a ‘smoothed’ cAMP signal in the face of variable intracellular Ca^{+2} . Another possibility is that AC3 itself may be involved in the generation of Ca^{+2} oscillations in IMCD cells upon hormonal stimulation. HEK-293 cells stably expressing AC3 produced Ca^{+2} oscillations with a periodicity of 3–5 min upon stimulation with glucagon, isoproterenol, or forskolin (45).

There is also evidence that Ca^{+2} -CaM can indirectly *inhibit* AC3 via activation of a specific calmodulin-dependent kinase, CaM kinase II, which phosphorylates AC3 inhibiting its cyclase activity (46;47). Inhibition of AC3 activity through CaM kinase II-mediated phosphorylation may provide a critical switch in terminating cAMP-mediated signaling in the collecting duct. For instance, inhibition of AC3 may hold relevance in the phenomenon of escape from vasopressin-induced antidiuresis seen in the clinical syndrome of inappropriate antidiuresis (SIADH) in which cAMP activity and aquaporin-2 expression undergo marked decreases despite high levels of circulating vasopressin (48).

Aside from AC3 and AC6, our RT-PCR studies indicate that other AC isoforms are expressed in the IMCD, namely AC2, 4, 5, 7, and 9. Further studies would be required to pinpoint the functional role of these isoforms.

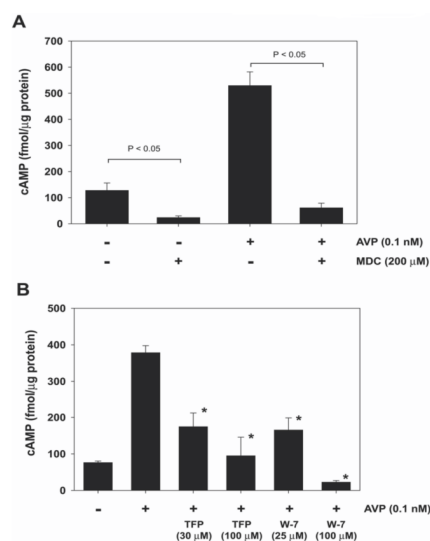
We have identified at least two sites of calmodulin action in the regulation of AQP2 in the IMCD, viz. MLCK (3) and AC3 (this paper). Given the multiplicity of its actions in cells, calmodulin likely plays other physiologically significant roles in the IMCD. One such role is stimulation of phosphodiesterase (PDE) activity which has been demonstrated in prior studies (49;50). The potential attenuation of the cAMP response via CaM-sensitive PDE-1 has not been addressed in this study. Inclusion of the PDE inhibitor IBMX prior to measurement of cAMP precluded evaluation of CaM-sensitive PDE activity.

In conclusion, we have demonstrated CaM-dependent cAMP accumulation in response to AVP in IMCD and have provided evidence for AC3 as the adenylyl cyclase isoform that is responsible for this activity. Calmodulin-stimulated adenylyl cyclase activity may play a critical role in the fine regulation of water and urea transport in the IMCD.

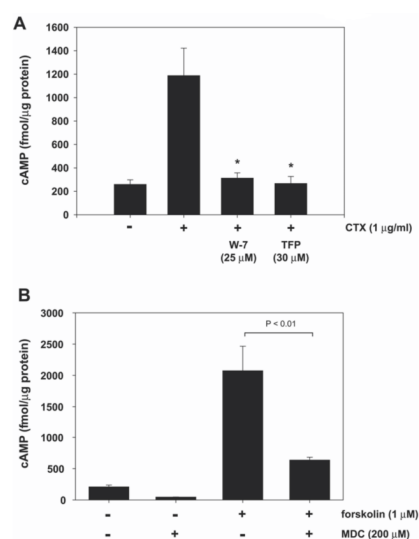
References

1. Knepper MA, Nielsen S, Chou CL, DiGiovanni SR. *Semin. Nephrol* 1994;14:302–321. [PubMed: 7938946]
2. Chou CL, Yip KP, Michea L, Kador K, Ferraris JD, Wade JB, Knepper MA. *J. Biol. Chem* 2000;275:36839–36846. [PubMed: 10973964]
3. Chou CL, Christensen BM, Frische S, Vorum H, Desai RA, Hoffert JD, de LP, Nielsen S, Knepper MA. *J. Biol. Chem* 2004;279:49026–49035. [PubMed: 15347643]
4. Katsura T, Verbavatz JM, Farinas J, Ma T, Ausiello DA, Verkman AS, Brown D. *Proc. Natl. Acad. Sci. U. S. A* 1995;92:7212–7216. [PubMed: 7543677]
5. Grantham JJ, Burg MB. *Am. J. Physiol* 1966;211:255–259. [PubMed: 5911047]
6. Zhang C, Sands JM, Klein JD. *Am. J. Physiol Renal Physiol* 2002;282:F85–F90. [PubMed: 11739116]
7. Morris RG, Schafer JA. *J. Gen. Physiol* 2002;120:71–85. [PubMed: 12084777]
8. Ausiello DA, Hall D. *J. Biol. Chem* 1981;256:9796–9798. [PubMed: 7275976]
9. Takaichi K, Kurokawa K. *Am. J. Physiol* 1988;255:F834–F840. [PubMed: 2847548]
10. Star RA, Nonoguchi H, Balaban R, Knepper MA. *J. Clin. Invest* 1988;81:1879–1888. [PubMed: 2838523]
11. Defer N, Best-Belpomme M, Hanoune J. *Am. J. Physiol Renal Physiol* 2000;279:F400–F416. [PubMed: 10966920]
12. Xia Z, Choi EJ, Wang F, Storm DR. *Neurosci. Lett* 1992;144:169–173. [PubMed: 1436697]
13. Defer N, Marinx O, Poyard M, Lienard MO, Jegou B, Hanoune J. *FEBS Lett* 1998;424:216–220. [PubMed: 9539154]
14. Chaudhry A, Muffler LA, Yao R, Granneman JG. *Am. J. Physiol* 1996;270:R755–R760. [PubMed: 8967404]
15. Mhaouty-Kodja S, Bouet-Alard R, Limon-Boulez I, Maltier JP, Legrand C. *J. Biol. Chem* 1997;272:31100–31106. [PubMed: 9388262]
16. De LV, Melino G. *Mol. Cell Biol* 2001;21:148–155. [PubMed: 11113189]
17. Terris J, Ecelbarger CA, Nielsen S, Knepper MA. *Am. J. Physiol* 1996;271:F414–F422. [PubMed: 8770174]
18. Nielsen S, DiGiovanni SR, Christensen EI, Knepper MA, Harris HW. *Proc. Natl. Acad. Sci. U. S. A* 1993;90:11663–11667. [PubMed: 8265605]
19. Stokes JB, Grupp C, Kinne RK. *Am J Physiol* 1987;253:F251–F262. [PubMed: 3303974]
20. Chou CL, DiGiovanni SR, Luther A, Lolait SJ, Knepper MA. *Am J Physiol* 1995;269:F78–F85. [PubMed: 7631834]
21. Laemmli UK. *Nature* 1970;227:680–685. [PubMed: 5432063]
22. Davis JQ, Bennett V. *J Biol. Chem* 1984;259:13550–13559. [PubMed: 6092380]
23. Hoffert JD, van Balkom BW, Chou CL, Knepper MA. *Am. J. Physiol Renal Physiol* 2004;286:F170–F179. [PubMed: 12965894]
24. Cornwell MM, Juliano RL, Davies PJ. *Biochim. Biophys. Acta* 1983;762:414–419. [PubMed: 6133561]
25. Nishikawa M, Tanaka T, Hidaka H. *Nature* 1980;287:863–865. [PubMed: 7432502]
26. Sugden MC, Christie MR, Ashcroft SJ. *FEBS Lett* 1979;105:95–100. [PubMed: 226410]
27. Sundan A, Sandvig K, Olsnes S. *Biochem. Biophys. Res. Commun* 1983;117:562–567. [PubMed: 6318763]
28. Liu CY, Jamaledin AJ, Zhang H, Christofi FL. *Brain Res* 1999;826:253–269. [PubMed: 10224303]
29. Chabardes D, Firsov D, Aarab L, Clabecq A, Bellanger AC, Siaume-Perez S, Elalouf JM. *J. Biol. Chem* 1996;271:19264–19271. [PubMed: 8702608]
30. van Balkom BW, Hoffert JD, Chou CL, Knepper MA. *Am. J. Physiol Renal Physiol* 2004;286:F216–F224. [PubMed: 14532164]
31. Nielsen S, Knepper MA. *Am. J. Physiol* 1993;265:F204–F213. [PubMed: 8396342]
32. Nielsen S, Frokiaer J, Marples D, Kwon TH, Agre P, Knepper MA. *Physiol Rev* 2002;82:205–244. [PubMed: 11773613]

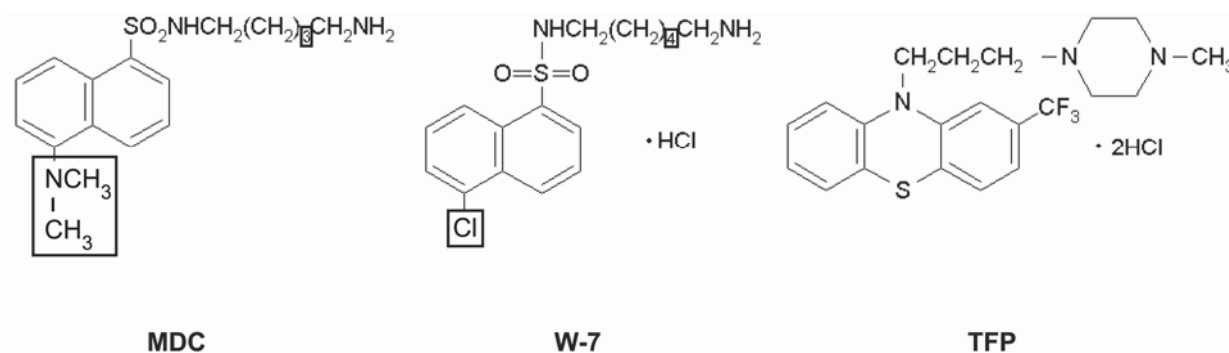
33. Nielsen S, Chou CL, Marples D, Christensen EI, Kishore BK, Knepper MA. Proc. Natl. Acad. Sci. U. S. A 1995;92:1013–1017. [PubMed: 7532304]
34. Inoue T, Terris J, Ecelbarger CA, Chou CL, Nielsen S, Knepper MA. Am. J. Physiol 1999;276:F559–F566. [PubMed: 10198415]
35. Stewart GS, Fenton RA, Wang W, Kwon TH, White SJ, Collins VM, Cooper G, Nielsen S, Smith CP. Am. J. Physiol Renal Physiol 2004;286:F979–F987. [PubMed: 15075194]
36. Helies-Toussaint C, Aarab L, Gasc JM, Verbavatz JM, Chabardes D. Am. J. Physiol Renal Physiol 2000;279:F185–F194. [PubMed: 10894801]
37. Cooper, D. M., Yoshimura, M., Zhang, Y., Chiono, M., and Mahey, R. (1994) *Biochem. J.* **297** (Pt 3), 437–440
38. Katsushika S, Chen L, Kawabe J, Nilakantan R, Halnon NJ, Homcy CJ, Ishikawa Y. Proc. Natl. Acad. Sci. U. S. A 1992;89:8774–8778. [PubMed: 1528892]
39. Nickols HH, Shah VN, Chazin WJ, Limbird LE. J. Biol. Chem 2004;279:46969–46980. [PubMed: 15319442]
40. Choi EJ, Xia Z, Storm DR. Biochemistry 1992;31:6492–6498. [PubMed: 1633161]
41. Mamluk R, Defer N, Hanoune J, Meidan R. Endocrinology 1999;140:4601–4608. [PubMed: 10499516]
42. Ecelbarger CA, Chou CL, Lolait SJ, Knepper MA, DiGiovanni SR. Am. J. Physiol 1996;270:F623–F633. [PubMed: 8967340]
43. Imbert-Teboul M, Champigneulle A. C. R. Seances Soc. Biol. Fil 1995;189:151–167. [PubMed: 8590215]
44. Yip KP. J. Physiol 2002;538:891–899. [PubMed: 11826172]
45. Wayman GA, Hinds TR, Storm DR. J. Biol. Chem 1995;270:24108–24115. [PubMed: 7592612]
46. Wei J, Wayman G, Storm DR. J. Biol. Chem 1996;271:24231–24235. [PubMed: 8798667]
47. Wei J, Zhao AZ, Chan GC, Baker LP, mpey S, Beavo JA, Storm DR. Neuron 1998;21:495–504. [PubMed: 9768837]
48. Ecelbarger CA, Chou CL, Lee AJ, DiGiovanni SR, Verbalis JG, Knepper MA. Am. J. Physiol 1998;274:F1161–F1166. [PubMed: 9841509]
49. Kusano E, Yoshida I, Takeda S, Homma S, Yusufi AN, Dousa TP, Asano Y. Tohoku J. Exp. Med 2001;193:207–220. [PubMed: 11315768]
50. Yamaki M, McIntyre S, Rassier ME, Schwartz JH, Dousa TP. Am. J. Physiol 1992;262:F957–F964. [PubMed: 1320333]

**Fig. 1.**

CaM inhibitors significantly reduce AVP-stimulated cAMP accumulation in isolated IMCD suspensions. A: Preincubation of tubules with MDC (200 μ M) completely blocked the elevation of cAMP by vasopressin (AVP) (0.1 nM). MDC also significantly reduced baseline cAMP levels in the absence of AVP. Levels of cAMP are expressed as fmol cAMP per μ g of total protein ($n \geq 3$; $P < 0.05$). B: Preincubation of tubules with either TFP or W-7 resulted in a dose-dependent inhibition of AVP-stimulated cAMP ($n \geq 3$; *, $P < 0.01$).

**Fig. 2.**

Effect of CaM inhibitors on CTX and forskolin-stimulated cAMP accumulation. A: IMCD suspensions were preincubated for 10 min in the presence or absence of two different CaM inhibitors, W-7 (25 µM) or TFP (30 µM), and then incubated with CTX (1 µg/ml) for 45 min and cAMP measured (n = 4; * P < 0.01 vs. CTX alone). CaM inhibitors blocked elevation of cAMP produced by CTX. B: IMCD suspensions were preincubated with either DMSO (–) or MDC (+) (200 µM) for 10 min followed by a 5 min incubation in the presence or absence of forskolin (1 µM). MDC blocked forskolin-stimulated cAMP accumulation (n = 3; P < 0.01).

**Fig. 3.**

Structural formulas of the three CaM inhibitors used in this study. There is high structural similarity between MDC and W-7 (Differences are boxed). Both MDC and W-7 have been reported to inhibit transglutaminase.

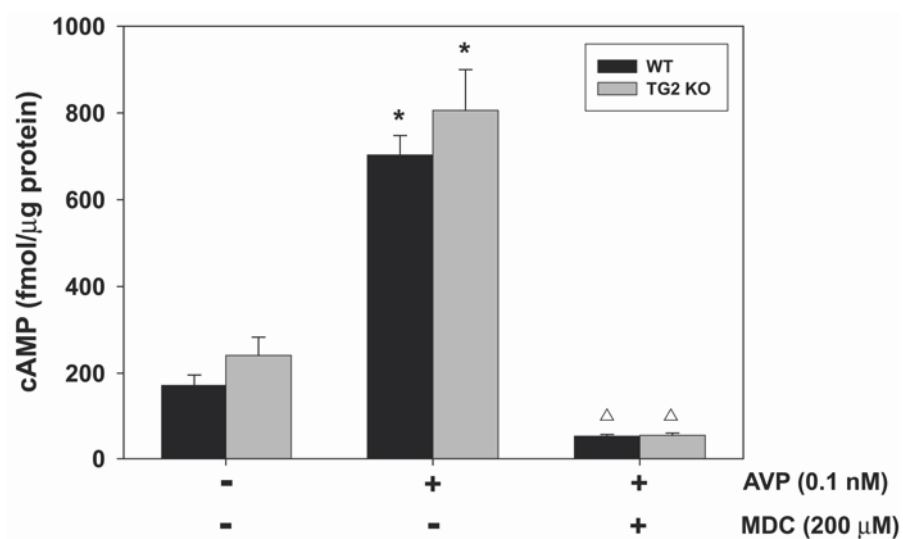
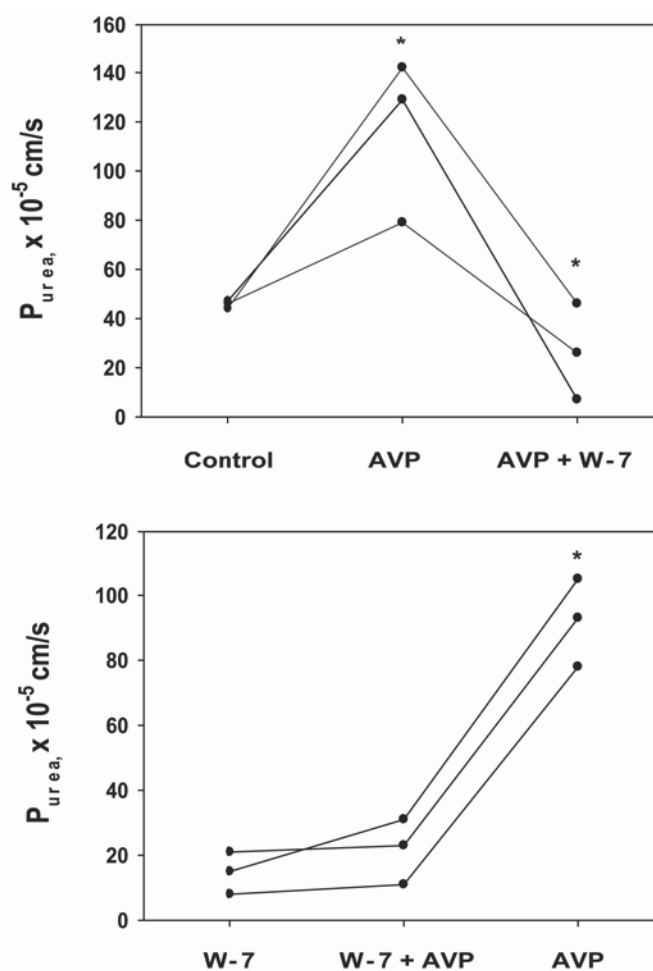
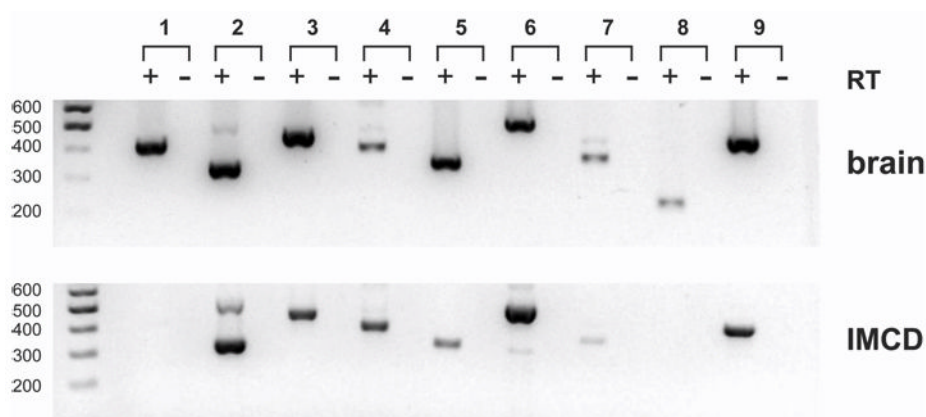


Fig. 4.
Effect of MDC on cAMP accumulation in wildtype (WT) and transglutaminase 2 (TG2) knockout mice. MDC inhibits AVP-stimulated cAMP accumulation in both WT and TG2 (-/-) mice. (, P < 0.001 vs. no AVP; Δ, P < 0.001 vs. AVP alone).*

**Fig. 5.**

Effect of CaM inhibitor W-7 on urea permeability of isolated perfused IMCD segments. After initial equilibration of tubules at 37°C for 30 min, P_{urea} was measured in three experimental periods: Control, AVP, and AVP+ W-7 (*Top panel*); W-7, W-7+AVP, and AVP (washout of W-7) (*Bottom panel*). Urea permeability was determined at 20 min after incubation with the reagent(s) in each period. AVP was used at 10^{-10} M concentration and W-7 was used at 25 μM concentration. All reagents were added into the peritubular bath solution. Values are mean \pm SE, $n = 3$ in each group; *, significantly different from previous experimental period ($P < 0.01$).

**Fig. 6.**

RT-PCR analysis of adenylyl cyclase isoforms in rat brain and IMCD. Total RNA was extracted from both brain and enriched IMCD suspensions and used for RT-PCR analysis with specific primers to each adenylyl cyclase (AC) isoform (1–9). Reactions without reverse transcriptase (RT –). Brain was chosen as a positive control for all primer sets. The CaM-sensitive isoform (AC3) is present in IMCD cells, while the other CaM-sensitive isoforms, AC1 and 8, are absent.

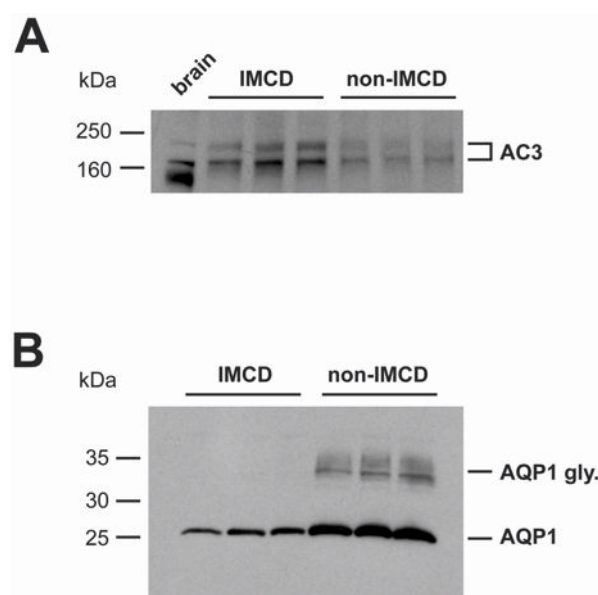


Fig. 7. *AC3 is enriched in rat IMCD fractions.* Rat inner medulla was processed according to *Methods* and differential centrifugation was performed to isolate IMCD and non-IMCD fractions. Immunoblotting followed by quantitation of band density was performed to determine level of enrichment. A. Immunoblot of AQP1 showing 5.4-fold enrichment in non-IMCD vs. IMCD fractions ($n = 3$; $P < 0.001$). B. Immunoblot of AC3 showing 2.2-fold enrichment in IMCD vs. non-IMCD fractions.

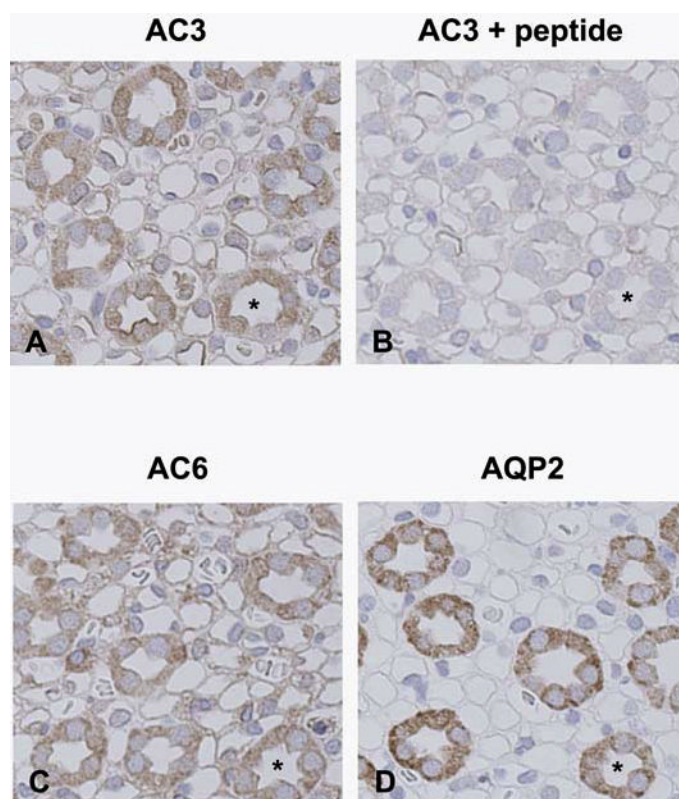


Fig. 8.

Immunoperoxidase labeling of AC3 and AC6 in rat inner medulla. Rat inner medulla was stained using antibodies to AC3 (A), AC3 preadsorbed with blocking peptide (B), AC6 (C), and AQP2 (D). AC3 and AC6 are both present in IMCD cells. AQP2 was used as a collecting duct-specific marker. Representative collecting ducts are indicated with an asterisk (*).

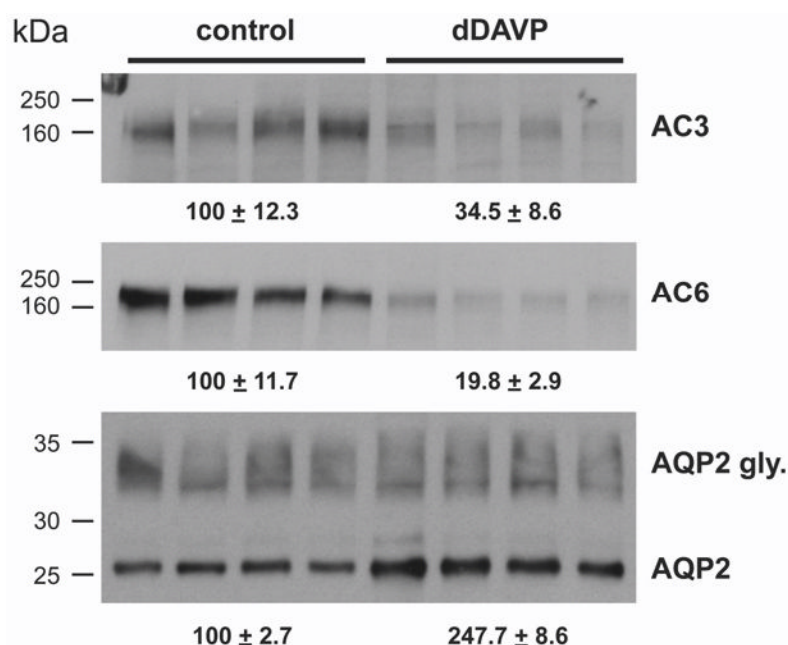


Fig. 9. Both AC3 and AC6 expression are decreased with long-term dDAVP treatment. Brattleboro rats were given dDAVP (20 ng/hr) or saline (control) via osmotic minipumps for 7 days, followed by isolation of inner medulla and immunoblotting (n = 4). Blots were probed with antibody to AC3 (top panel), AC6 (middle panel), or AQP2 (bottom panel).